Spring 5-11-2012

Photoionization Cross Section Measurement of Rb 5P3/2

Charles Young
University of Southern Mississippi

The University of Southern Mississippi

Photoionization Cross Section Measurement of Rb $5P_{3/2}$

by

Charles Young

A Thesis

Submitted to the Honors College of
The University of Southern Mississippi
In Partial Fulfillment
Of the Requirements for the Degree of
Bachelor of Science
in the Department of Physics and Astronomy

February 2012

Approved by

_____

Dr. Alina Gearba
Professor of Physics and Astronomy

_____

Dr. Khin Maung Maung, Chair
Department of Physics and Astronomy

_____

Dr. David R. Davies, Dean
Honors College

ACKNOWLEDGEMENTS

The author would like to thank Dr. Alina Gearba for being a great mentor, teacher, and catalyst throughout their interaction. This process has been hectic at times, but it should not be altered in any way. Special thanks are extended to Brad Crochet, Dr. Gearba's Ph.D. student, for thoroughly explaining the function of each piece of equipment in the laboratory as well as serving as a guide throughout the entire experiment. This research was supported by the Undergraduate Research award provided by Sigma Pi Sigma and the Atomic Molecular and Optical Physics program of the National Science Foundation. The author was supported by the Presidential Scholarship awarded by the Honors College. The scholarship has been invaluable in my pursuit of a degree, providing a conducive study environment and allowing a greater concentration for physics. Without the support from my wife, Haley Young, I would not have been able to accomplish nearly as much during my study at the University of Southern Mississippi.

Table of Contents

Background

The photoionization of atoms is still an emerging field with a foundation in laboratories and journals, yet much in the field is unknown. Photoionization is the phenomenon of an incident photon on a gaseous atom causing the ejection of an electron, and therefore, the atom becomes an ion. The photoelectric effect is a similar but broader term dealing with atoms in all forms: solid, liquid, gas, and plasma. The photoelectric effect causes a current whenever light with a certain wavelength is shined on a metal. The wavelength that is needed to eject an electron is dependent on the atom(s) involved and the state that atom is in. The photons will free electrons, which can be used to power devices. Examples can be seen in photocells and solar cells [1]. Photocells can detect light through the photoelectric effect by producing a current. They are common in photodiodes, photomultiplier tubes, and night vision devices. Solar cells convert light into electrical energy and can be seen in solar powered calculators, cars, lights, and other solar powered devices.

Unlike the photoelectric effect, photoionization only applies to gaseous atoms. The photoionization of atoms is a useful method within the research community since it can be used to determine the binding energy of electrons [2] and in photo-emission spectroscopy, but it also has more practical applications such as in photoionization detectors, the most efficient and least expensive gas detector [3], and in creating plasma [4]. Plasma is a form of matter consisting of positively charged ions and its counterpart, free electrons. Plasma is useful in cutting structural steel, in popular light sources, and in some gas lasers such as our Krypton-Argon ion laser [5]. Our Krypton-Argon ion laser is a product of past research within the area of photoionization; we are using a product of

the research advancements in photoionization to further explore the area of photoionization.

Specifically, we have experimentally determined several photoionization cross sections of the Rubidium. The photoionization cross section is related to the probability that an electron will be ejected from an atom due to the energy gained from incident photons. In our case, we are specifically concerned with the probability that an electron will be ejected from a Rubidium atom in the $5P_{3/2}$ excited state due to incoming photons with a known energy. This cross section is dependent on the wavelength of the ionizing photon [6]. We have measured four different photoionization cross sections by using photons with four different wavelengths and, therefore, four different energies.

Theoretical values have been computed for the total cross section of the 5P state by Aymar *et al.* at the threshold of 479 nm ranging from 1.25×10^{-17} cm^2 to 1.40×10^{-17} cm^2 [6]. This cross section is not a constant value, since it is dependent on the wavelength of the ionizing laser [6]. This dependence was determined to be nonlinear; however, the shape of the cross section versus wavelength is not yet known. For this reason, we have measured four different cross sections. The final goal would be to determine the shape of the photoionization cross section versus wavelength, but that would require knowing many cross sections at different wavelengths. Our laser, an Innova 70C Spectrum Ion Argon-Krypton Laser, can operate at wavelengths of 457.9, 465.8, 472.2 and 476.5 nm which are below the ionization threshold of 479.1 nm. We have measured photoionization cross sections at these wavelengths. The photoionization cross section at 476.5 nm has already been experimentally determined by Gabbanini *et al.* to be $1.48\ (22) \times 10^{-17}$ cm^2 [7]. One of our objectives is to experimentally arrive at a value similar to Gabbanini's to reassure that our method is accurate. Our second objective is to determine three other cross sections at wavelengths 457.9, 465.8, and

472.2 nm since these wavelengths are generated by our laser and the cross section has not yet been determined for them. In order to calculate the cross sections at these wavelengths, we have measured the photoionization rate of trapped atoms and taken into account the $5P_{3/2}$ excited state fraction.

The use of trapped Rubidium atoms to measure photoionization cross sections was first performed by Dinneen *et al.* [8]. By utilizing trapped atoms in a magneto-optical trap (MOT), he was able to determine the photoionization cross section of Rb $5P_{3/2}$ at wavelengths 413 and 407 nm. Our values should match other published data and also provide new data that will contribute to determining the dependence of the photoionization cross section on the incident photon energy.

Theory

Dinneen *et al.* first described the method of determining photoionization cross sections through the use of laser traps [8]. They applied this technique to Rubidium at the $5P_{3/2}$ state. They measured two photoionization cross sections to be 1.36 (12) x 10^{-17} and 1.25 (11) x 10^{-17} cm^2 for wavelengths of 413 and 407 nm, respectively [8]. These values are within the theoretical values predicted by Aymar *et al.* [6]. This data concurs with the fact that the photoionization cross section is dependent on the wavelength. However, since there are only two wavelength values, a precise comparison cannot be made.

Gabbanini *et al.* utilizes a similar method used by Dinneen *et al.* in measuring the photoionization cross section [7]. He notes that this method has advantages over previous methods of collecting ions since there is no need to calibrate the ion detection apparatus. Gabbanini's method does not need to take into account the absolute excited state density. On the other hand, Dinneen used a vapor cell trap; hence he has to measure the excited state density. The magneto-optical trap approach used by Gabbanini is very similar to what we are using to measure photoionization cross sections in the Laser Cooling and Trapping Laboratory at the University of Southern Mississippi.

Magneto-Optical Trap

The first step involves having a working magneto-optical trap that traps Rubidium atoms in the $5P_{3/2}$ state. Wieman *et al.* [9] provide much information regarding magneto-optic traps. The process of trapping atoms in a vapor cell trap is known as laser cooling and trapping. It involves three polarized laser beams to cool the atoms, a magnetic field to trap the atoms, a vacuum chamber to prevent unwanted interaction, and an atom

source. Only select atoms, such as those in the first column of the periodic table, Rubidium being one, can be cooled and trapped through this method [9].

The cooling process used by Wieman *et al.* [9] is known as Doppler cooling or optical molasses because it utilizes the Doppler effect to slow the atoms by having the photons absorb the atoms' kinetic energy. Three laser beams are configured to pass through a spot inside a vacuum chamber and are retro-reflected to create six total laser beams. The lasers must be detuned to a frequency below the resonance frequency. When a photon from the laser is scattered off of an atom, the atom will receive a small momentum kick. The cooling of the atoms is possible by forcing the rate that photons scatter off of atoms dependent on the velocity of the atom. Atoms that move against the direction of the laser will see the laser's frequency Doppler shifted closer to resonance, and experience a greater momentum kick against its velocity than atoms moving in the same direction of the laser. Since each laser beam is directly overlapped by a beam counter propagating in the opposite direction, the atom will always lose kinetic energy when in the path of a laser. This will cool the atoms to temperatures in the micro Kelvin region by removing most of their momentum and kinetic energy [9].

Doppler cooling alone does not provide a continuous sample of cold Rubidium atoms. Now that the atoms are cooled, they must be trapped in one spot since they will still slowly move out of the trap. When a force was needed that would slow the atoms down, the force had to be velocity dependent. Now, a force is needed to hold the atoms in one particular location, so the force must be position dependent. An inhomogeneous magnetic field along with the polarization of the laser beams will create this position dependent force [9]. Gabbanini *et al.* [7] utilizes a magnetic field created by a pair of

coils aligned in anti-Helmholtz configuration along the z-axis (vertical). The coils are positioned above and below the MOT. Both coils must have opposite parity or current to create a magnetic field that is zero at the MOT location and increases the further away from the MOT an atom is. The shifts in atomic energy levels caused by the magnetic field are known as Zeeman shifts. The position dependent force acts just like the velocity dependent force: the further an atom is from the point of zero magnetic field, the more it is pulled toward that point [9]. This position dependent force will trap the atoms in one place, creating a dense sample of cold Rubidium atoms that we can use for our experiment.

Wieman *et al.* [9] use a MOT to cool and trap a source of Rubidium atoms with the use of six tuned polarized lasers that Doppler cool the atoms and a magnetic field that traps the atoms inside a vacuum chamber. The vacuum chamber ensures that minimum background gases will interact with the MOT. The lasers must be tuned and stabilized directly below the transition level to ensure MOT existence and stability. Wieman *et al.* use saturated absorption spectroscopy to stabilize and lock the lasers to the required frequency [10].

Doppler-free Saturated Absorption Spectroscopy

In order to achieve a magneto-optical trap, the lasers used must be operating within a stabilized frequency. This can be accomplished through the use of Doppler-free saturated absorption spectroscopy. Preston [10] provides a thorough paper that explains the usefulness of Doppler-free saturated absorption spectroscopy in Rubidium to stabilize lasers to within particular frequency. It requires three separate laser beams originating

from the same laser, a Rubidium vapor cell, two photodiodes, and miscellaneous optics to separate the laser into three parts and direct it into the cell.

The laser beam can be divided into three parts by the use of a beam splitter. The most intense beam is labeled the "pump" beam. The other two beams are called "probe" beams. One probe beam is sent through the cell in the opposite direction that the pump beam travels. It is aligned to overlap the pump beam, and is therefore the "overlap" beam of the two probe beams. The other probe beam, known as the "reference" beam passes through the cell without overlapping any beam. Both probe beams are monitored by a photodiode after passing through the cell.

Preston [10] notes that the difference of the two signals is the overall goal of Doppler free saturated absorption spectroscopy. The absorption signal that comes from the reference beam will display Doppler broadened absorption lines due to the atoms having a distribution of velocities. The pump beam will deplete the source of atoms in the ground state, causing the overlap beam to absorb fewer atoms than its counterpart reference beam. The absorption signal that comes from the overlap beam will therefore display reduced absorption. When these two signals are subtracted from one another, the resulting signal will have Doppler-free saturated absorption peaks. This is due to one signal having full peaks, while the other has peaks with dips at the hyperfine transitions. Therefore, when the two signals are subtracted, the resulting signal has no Doppler structure and displays only the peaks corresponding to the hyperfine transitions. A lock-in amplifier can then be used to lock the laser frequency to one of these peaks. By this method the laser will be sufficiently stable at this frequency to provide conditions suitable for a MOT.

Photoionization Cross Section Measurement

Knowing the number of excited state atoms in the MOT is a necessity of this method of determining the photoionization cross section of Rubidium. This can be determined by measuring the fluorescence of the atoms as they return to the ground state from the $5P_{3/2}$ state. This loss rate is simply the rate that atoms are leaving the trap. Gabbanini *et al.* [7] states that the loss rate of the vapor cell trap without the ion beam irradiating is due to atoms in the trap colliding with the background gases and colliding with other atoms in the vapor cell trap. Therefore, he gives the loss rate without the ion beam to be

$$R_L = R_{Lb} + \beta_c f n \qquad (1)$$

where the first term is due to collisions with background gases and the second term is due to collisions with other atoms in the trap. The second term can be neglected since these collisions are negligible compared to background gas collisions.

If another variable is introduced that causes additional loss of atoms in the vapor cell trap, then a new loss rate is must be computed. When photoionization is an added variable, the new loss rate is

$$R'_L = R_L + \frac{I_{PI}}{E_{PI}} f \sigma_{PI} \qquad (2),$$

where R_L is the loss rate without photoionization and the second term takes account for the loss rate due to photoionization. I_{PI} is the ion laser intensity, E_{PI} is the photon energy, f is the excited state fraction, and σ_{PI} is the photoionization cross section. When these two loss rates are subtracted, the result is the loss rate due to only photoionization [7].

The characteristics of the vapor cell trap with the ion beam irradiating it can now be described as

$$N(t) = N_o'[1 - e^{-R_L' t}] \qquad (3),$$

where N(t) is the number of atoms in the trap as a function of time. By this function, before the vapor cell trap begins to load, the number of atoms in the trap N(t) is zero. As the trap loads, the number of atoms in the trap increases. The number of atoms will eventually reach a plateau, N_o' after much time has passed [7].

The characteristics of the vapor cell trap without ionization as a loss rate can be described similarly as

$$N(t) = N_o[1 - e^{-R_L t}] \qquad (4),$$

where R_L is the loss rate due to collisions with other gases. This function behaves similarly to the function in equation (4), but it has a different plateau, at N_o as time increases, and it will have a slightly different shape to the curve due to Euler's constant being raised to a different power.

By measuring the loss rate strictly due to photoionization, Gabbanini *et al.* [7] was able to determine the photoionization cross section. The only unknown variables in equation (2) are the photon energy, the excited state fraction, and the ion laser intensity. These variables can also be measured.

Excited State Fraction of Rb at $5P_{3/2}$

The excited state fraction can be determined using an expression derived for a simple two-level atom [11]:

$$f = \frac{I_T/I_S}{1 + 2I/I_S + (2\delta/\Gamma)^2} \qquad (5)$$

where I_T is the total intensity in the six trapping beams, δ is the detuning of the trapping laser frequency from resonance, Γ is the natural linewidth of the transition and I_S is the

saturation intensity. This has been confirmed to work for our particular situation with a magneto-optical trap by Shah *et al.* [11]. Also, the photon energy can be calculated knowing the wavelength of the ion laser, and the ion laser intensity can be determined by measuring the power and area of the ion laser beam.

Gabbanini *et al.* measured the photoionization cross section of Rb at the $5P_{3/2}$ to be 1.48×10^{-17} cm^2 at a wavelength of 476.5 nm [7]. This is near other theoretical and experimental values. Klyucharev and Sepman, who used a different method than trapped atoms, measured a photoionization cross section of 9.8×10^{-18} cm^2 at 444 nm in 1975 [12].

Experimental Procedure

In order to measure the cross section, we set up a Magneto-Optical Trap of Rubidium atoms. This preliminary phase has already been completed in our lab from previous research. In the first stage of our laser beam path, we have used Doppler-free saturated absorption spectroscopy to stabilize the two lasers' frequency. We shifted the trapping laser's frequency up with an acousto-optic modulator in order to be closer to but just below resonance. We overlapped the two laser beams used for the MOT, the trapping laser and the pump laser. Then, by using quarter wave plates and beam-splitting cubes, we split the now one laser beam into six laser beams. From there, the separated laser beams pass through additional quarter wave plates allowing us to change their polarization. Four beams are sent through the vacuum chamber at a horizontal through different windows, while the last two beams are sent through the vacuum chamber on the vertical axis. A pair of coils in anti-Helmholtz configuration surrounds the chamber and is monitored by a highly precise power supply. Our vacuum pressure will be maintained by a roughing pump and a turbo pump and monitored by our vacuum pressure gauge. The Rubidium getters are then turned on to allow Rubidium into the chamber. Through this process, we have attained a MOT of Rubidium atoms.

Once a stable MOT has been created, the fluorescence from the atoms trapped in the MOT versus time is measured with a photomultiplier tube by capturing the photons that are emitted from electrons returning to the ground state as the MOT loads. The background fluorescence is also measured in order to prevent ambient light and laser light from interfering and skewing our data. After we plotted the fluorescence emitted by the atoms in the MOT versus time while the ionizing beam is off, we determine the loss

rate of the MOT from equation (4). Likewise, once we plot the fluorescence emitted by the atoms in the trap versus time while the ionizing beam is irradiating the trap, we determine the loss rate of the MOT from equation (3). Subtracting these two loss rates yields the loss rate of atoms in the trap only due to photoionization. This is how we measured the loss rate due to only photoionization.

According to Equation (2),

$$R'_L - R_L = \frac{I_{PI}}{E_{PI}} f \sigma_{PI} \qquad (6)$$

where R'_L is the loss rate with photoionization, R_L is the loss rate without photoionization, I_{PI} is the ion laser intensity, E_{PI} is the photon energy, f is the excited state fraction, and σ_{PI} is the photoionization cross section. The ion laser intensity at the MOT is calculated by measuring the intensity and area of the ion laser before and after the MOT while taking into account losses due to two windows it passes through. The photon energy is calculated knowing the wavelength of the ion laser. The excited state fraction is calculated from Equation (5). We manipulate Equation (2) to yield the photoionization cross section at that particular wavelength. We have repeated this procedure for each of the four wavelengths we planned to measure the photoionization cross section.

Results

In order to measure the loss rates of the MOT, we first plot the loading curves of the MOT on a fluorescence versus time graph. Typical loading curves can be seen in Figure 1. The red data points are fluorescence from the MOT loading without the ion laser on, while the green data points are fluorescence from the MOT loading with the ion laser on. The figure only represents one photoionizing wavelength and intensity: 476.5 nm and 350 mW/cm^2. The solid lines within the fluorescence data points are fits used to determine the loss rates according to equations (3) and (4).

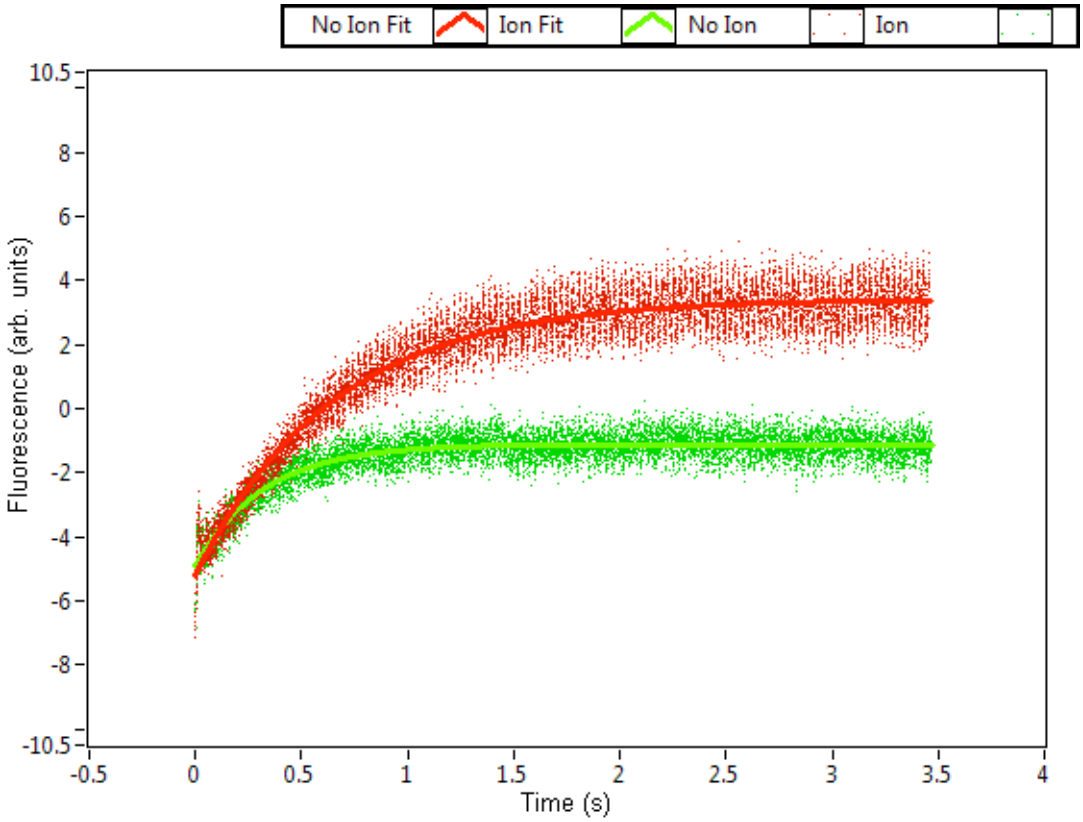

Fig. 1

Since this data is only representative of one wavelength and one intensity of our photoionizing laser, we must repeat this procedure many times to reduce the uncertainty

in the loss rate measurement. In order to get an accurate cross section measurement, we record the loading curves for several different intensities of the photoionizing laser. Also, our purpose is to determine the cross section for four different photoionizing wavelengths. This required us to repeat the entire procedure four different times. After determining the loss rates from the fits, we subtract the two rates to yield the loss rate due to only photoionization for that intensity and at that particular photoionizing wavelength. Figure 2 exhibits the photoionization loss rate versus photoionizing intensity. It can readily be seen that the relationship is linear, as it should be. The solid line is the straight line fit of the data points.

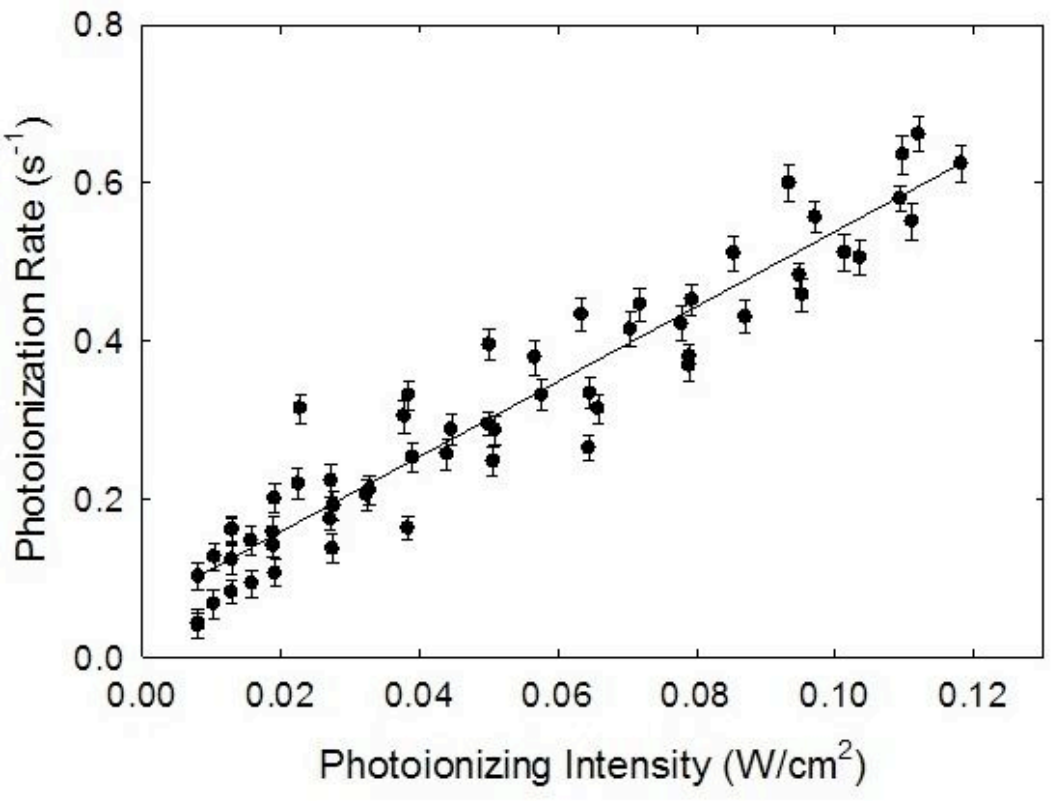

Fig. 2

It can be seen from equation (2) that the slope of the line is proportional to the photoionization cross section and the excited state fraction and inversely proportional to the photon's energy. For our experimental parameters, equation (5) gives an excited state fraction of f = 0.21(2). We can calculate the photon's energy from

$$E = \frac{hc}{\lambda},$$

where h is Planck's constant, c is the speed of light, and λ is the photoionizing wavelength. The photoionization cross-section of the Rb $5P_{3/2}$ excited state at 476.5 nm is calculated to be 9.45(98) x 10^{-18} cm^2, which is about 30% lower than the value of 1.48(22) x 10^{-17} cm^2 reported in Ref. [7].

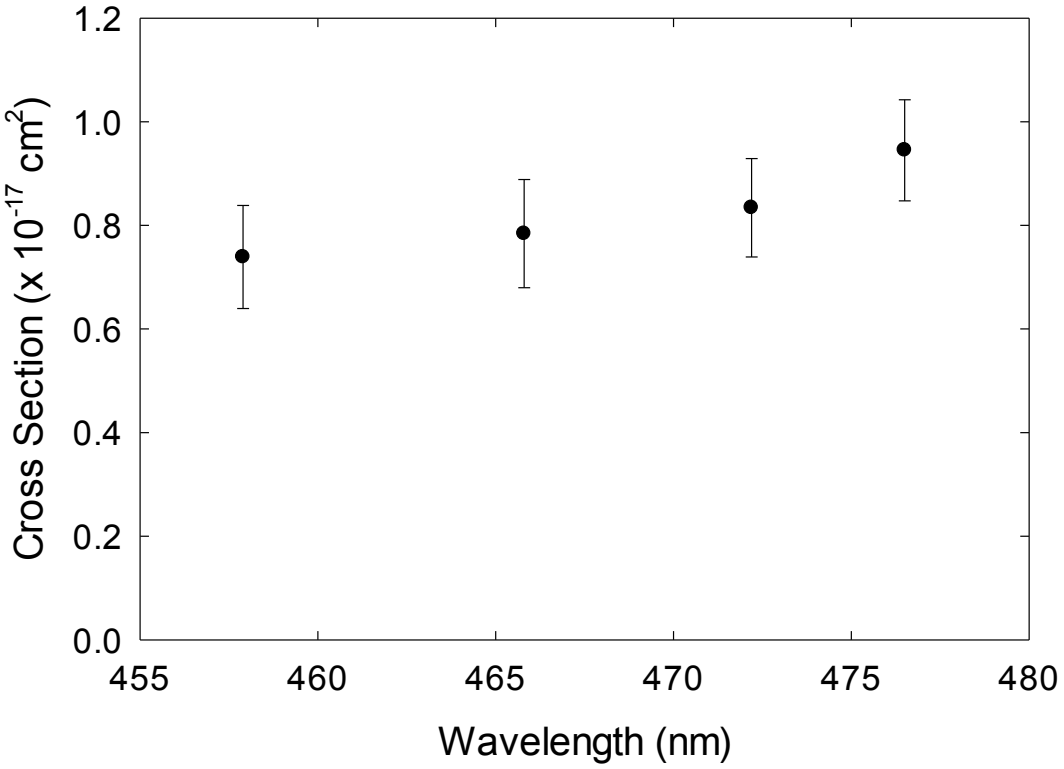

Fig. 3

Figure 3 displays the photoionization cross sections that we computed for the wavelengths 457.9, 465.8, 472.2, and 476.5 nm. For the photoionizing wavelength 457.9 nm, we computed a cross section of 7.39(99) x 10^{-18} cm^2. We computed a cross section of 7.84(104) x 10^{-18} cm^2 for the photoionizing wavelength 465.8 nm. For the photoionizing wavelength 472.2 nm, we computed a cross section of 8.34(95) x 10^{-18} cm^2. These last three cross sections have not been determined before. Our purpose is to determine cross sections for as many photoionizing wavelengths as possible in order to conclude the shape of dependence between the cross section and photoionizing wavelength.

Discussion

The uncertainty in determining the cross section takes into account statistical errors, as well as the uncertainty in the excited state fraction and the photoionizing intensity, given by the uncertainty in measuring the power and size of the ion laser beam. This can be seen from equation 6,

$$R'_L - R_L = \frac{I_{PI}}{E_{PI}} f \sigma_{PI} \qquad (6)$$

where any error in each of the terms will propagate into the total error in determining the cross section. The E_{PI} term's error is negligible since $E_{PI} = \frac{hc}{\lambda}$, where h is Planck's constant and c is the constant speed of light. Due to our photoionizing laser's specifications, we know the wavelength λ of the photoionizing beam to such a degree that the uncertainty from E_{PI} is negligible compared to other uncertainties. By using the definition of intensity as power per area, we determined the uncertainty in the photoionizing intensity to be

$$\frac{u\{I\}}{I} = \sqrt{\left(\frac{u\{P\}}{P}\right)^2 + \left(\frac{u\{r(x)\}}{r(x)}\right)^2 + \left(\frac{u\{r(y)\}}{r(y)}\right)^2}$$

where u{x} is the uncertainty in x, I is the photoionizing intensity, P is the power in Watts, r(x) is the elliptical major axis in meters, and r(y) is the elliptical minor axis in meters. This uncertainty in intensity contributes to the total uncertainty of the cross section. The excited state fraction's uncertainty contribution was determined to be

$$\frac{u\{f\}}{f} = (1 - 2f)\sqrt{\left(\frac{u\{I_T\}}{I_T}\right)^2 + \left(\frac{u\{I_S\}}{I_S}\right)^2 + \left[\frac{2(2\delta/\Gamma)^2}{1 + (2\delta/\Gamma)^2} * \left(\frac{u\{\delta\}}{\delta}\right)^2\right]}$$

where again u{x} is the uncertainty in x, f is the excited state fraction, I_T is the total intensity in the six trapping beams, I_S is the saturation intensity, δ is the detuning of the trapping laser frequency from resonance, and Γ is the natural linewidth of the transition. This expression can be derived from equation (5) by computing the partial derivatives of the excited state fraction with respect to each variable. A simplified version of the expression is

$$(u\{f\})^2 = (u\{I_T\})^2 \left(\frac{\partial f}{\partial I_T}\right)^2 + (u\{I_S\})^2 \left(\frac{\partial f}{\partial I_S}\right)^2 + (u\{\delta\})^2 \left(\frac{\partial f}{\partial \delta}\right)^2$$

The statistical errors from equation (6) originate from the fits of fluorescence data to equations (3) and (4) to determine R_L and R_L'. After the fit, that statistical error propagates through equation (6) to contribute to the total uncertainty in the cross section. For the cross section calculated at a photoionizing wavelength of 476.5 nm, the uncertainty is 0.98 x 10^{-18} cm^2. The uncertainties for wavelengths 457.9, 465.8, and 472.2 nm are 0.99 x 10^{-18} cm^2 , 1.04 x 10^{-18} cm^2, and 0.95 x 10^{-18} cm^2, respectively.

There is obviously some discrepancy between our results and previous experiments. Gabbanini *et al.* [7] calculated a cross section of 1.48(22) x 10^{-17} cm^2, which is larger by about 30% than our calculated cross section for the photoionizing wavelength of 476.5 nm. One cause for this discrepancy could be the way we defined our photoionizing intensity. We utilized the peak intensity to obtain our results, which is defined as twice the average intensity, which is just simply power per area. The size of our MOT is approximately ten times smaller than the size of the photoionizing laser beam. This is why we thought it would be best if we used the peak intensity: the MOT would most likely see the peak intensity instead of the average intensity.

Another explanation for the discrepancy between our results could be the excited state fraction. A MOT is a complicated system and different research groups use different simplified models to estimate their excited state fraction. In the near future we do plan on measuring the excited state fraction in our system and compare with the available theoretical models. We also plan on using a commercial beam profiler to check our measurements of the photoionizing laser beam size for consistency.

Conclusion

We have measured the photoionization cross section of the $5P_{3/2}$ excited state of laser-cooled rubidium at four wavelengths below the ionization threshold of 479 nm. Three of the four cross sections have not been previously measured. Our cross section at 476.5 nm is about 30% lower than previous measurements [7]. As expected, our data show that the photoionization cross section increases with the photoionizing wavelength. We plan on refining our experimental results by measuring directly the excited state fraction in the MOT and by using an alternate method for measuring the photoionizing laser beam size.

Bibliography

[1] "Photoelectric Effect." 2010. Science Clarified, Advameg, Inc. 27 October 2010. < http://www.scienceclarified.com/Oi-Ph/Photoelectric-Effect.html>.

[2] Demtröder, Wolfgang. *Atoms, Molecules and Photons*: An Introduction to Atomic-, Molecular-, and Quantum Physics. Heidelburg: Springer, 2010. Print.

[3] Pedrotti, Frank. *Introduction to Optics*. San Francisco: Pearson Addison Wesley, 2007. Print.

[4] "Resources." 2004. Plasmas International. 28 October 2010. <http://www.plasmas.com/topics.htm>.

[5] "Innova 70C: Technical Data." 2000. Coherent, Inc. 28 October 2010. <http://www.coherent.com/downloads/70CDatasheet.pdf>.

[6] *Central-field calculations of photoionisation cross sections of excited states of Rb and Sr^+ and analysis of photoionisation cross sections of excited alkali atoms using quantum defect theory.* M. Aymar, O. Robaux, and S. Wane, J. Phys. B: At. Mol. Phys. 17, 993 (1984).

[7] *Photoionization cross section measurement in a Rubidium vapor cell trap.* C. Gabbanini, S. Gozzini, A. Lucchesini, Opt. Comm. 141, 25 (1997).

[8] *Use of trapped atoms to measure absolute photoionization cross sections.* T. Dinneen, C. Wallace, K. Tan, and P. Gould, Opt. Lett. 17, 1706 (1992).

[9] *Inexpensive laser cooling and trapping experiment for undergraduate laboratories.* C. Wieman, G. Flowers, and S. Gilbert, Am. J. Phys. 63, 317 (1995).

[10] *Doppler-free saturated absorption: Laser spectroscopy.* D. Preston, Am. J. Phys. 64 1432 (1996).

[11] *Model-independent measurement of the excited state fraction in a magneto-optical trap*. M. Shah, H. Camp, M Trachy, G. Veshapidze, M. Gearba, and B. DePaola, Phys. Rev. A 75, 053418 (2007).

[12] *Two Stage Photoionization of Rubidium.* A. Klyucharev and V. Sepman, Opt. Spectrosc. 38, 712 (1975).